

# Automated Picking System Employing a Drone

Francesco Betti Sorbelli\*, Federico Corò†, Cristina M. Pinotti\* and Anil Shende‡

\*Dept. of Comp. Sci. and Math., University of Perugia, Italy Email: {francesco.bettisorbelli@unipg.it, cristina.pinotti@unipg.it}

†Gran Sasso Science Institute (GSSI), L'Aquila, Italy Email: federico.coro@gssi.it

‡Math., Comp. Sci. & Physics Dept. Roanoke College, VA, USA Email: shende@roanoke.edu

**Abstract**—We study the possibility of using drones to implement an automated picking system in a warehouse. We imagine a warehouse divided into two contiguous areas: in one area, the drone moves according to the Euclidean distance, while in the other area, the drone moves according to the Manhattan distance. For each customer-order (CO), the automated picking system is in charge of gathering the items requested in the CO to a predefined location where the cart of the drone is positioned. For each item of the order, the drone flies to the location where the item is stored, grasps it, and brings it back to its cart. Our goal is to find the position of the drone's cart that minimizes the sum of the distances traversed by the drone to pick-up all the items of the CO. We propose algorithms to find such a location when the items to be collected are in Euclidean and Manhattan areas. We can prove a  $\sqrt{2}$ -approximation factor for our solutions. Moreover, we compare the efficiency of the automated picking system employing a drone with that of a traditional picking system employing a worker that pushes a cart, and we find under which conditions the drone can be more efficient.

## I. INTRODUCTION

Drones or Unmanned Aerial Vehicles (UAVs) are recently becoming widely used in civil applications, e.g., environmental protection, public safety, localization [1], [2], and agriculture. Recently, there has also been an increasing interest in the use of drones on the stage of assembly of products [3]. Unit picking is labor-intensive, and the rise of e-commerce orders have intensified competition for efficient warehouse operations. Warehousing constitutes 30% of the cost of the logistics in the USA, and several theoretical perspectives that help supply chain decision-makers on determining when to invest in new robotics technology have been developed [4]. In this paper, we intend to investigate the use of drones for fulfillment of orders in warehouses.

### A. Current Technologies and Proposed Concepts

Some warehouse technology solutions are highly invasive and require building a warehouse from scratch. For example, the British supermarket Ocado uses robots to speed-up on-line grocery shopping [5]. Ocado's solution includes many robots of the size of a washing machine that wheel moving groceries on a structured ad-hoc warehouse where a giant chessboard-like floor, called "the hive", acts as the transport structure for the robots.

The work has been partially supported by GEO-SAFE (H2020-691161), "GNCS-INdAM", Project NALP-SAPR: *Navigazione Autonoma e Localizzazione Precisa per Sistemi Aeromobili a Pilotaggio Remoto* granted by FSE-Regione Umbria, and by Fondo Ricerca di Base 2018 University of Perugia.

Our research is instead oriented towards using drones for picking the objects: no transport structure is required because the drones fly, but the critical phase could be grabbing the items. However, in the near future, drones will likely be able to pick most forms of small items, for example, using, possibly foldable, robotic arms [6]–[8].

In our perspective, we foresee a drone that, for each item of the CO, after receiving from a central computer the location of the item to be picked and the predefined path to reach it, autonomously flies among the shelves as in Fig. 1(b), grabs the item, and drops it at the cart. The drone replaces the workers that pick the items as depicted in Fig. 1(a). A strength of the drone picking system is that it can be implemented in traditional warehouses without major infrastructure changes, perhaps only assuming that each item has an RFID tag as it is usual nowadays for loading and unloading of warehouses.

In the model adopted by this paper, there are two types of shelves in the warehouse: cabinets (see Fig. 1(a)), and open-racks (Fig. 1(c)). The cabinets are racks of shelves that have the back, but they do not have the doors, like those in Fig. 1(d). So the drone cannot cross them, but it can easily pick items from the front. The open-racks, instead, have no back and no door (see Fig. 1(c)), and they can be crossed by the drone. We assume that the shelves of the open-racks are kept partially filled so as the drone can fly throughout them.

In the warehouse, the cabinets and the open-racks form *lanes* (alias, *columns*), separated by aisles. Every cabinet or open-rack is logically partitioned in several *rows*. There is no aisle between two consecutive rows. Fig. 2 illustrates a view from the top of a warehouse with 10 lanes (6 low cabinets and 4 high open-racks) each consisting of 10 rows (row 1 is depicted in green). To move among the cabinets, the drone flies overhead and it can freely move from different points of different lanes. To move among the open-racks, the drone can move at different heights and passes among the open-racks. Since the open-racks have metallic pillars to support them, the drone cannot move from a row of a lane to a different row of another lane following a straight line; but it must follow the rows and the aisles. The possible 2D movements of the drone are shown by the blue dashed line in Fig. 2. Note that, instead, a human worker that pushes a cart has always to reach one of the two extremes of the lane to change the lane, as shown by the red dotted lines in Fig. 2.

Although the position of an item is given by the lane, the



Fig. 1: Different warehouse architectures.

row, and by the *height* of the shelf in the row, in this work, we consider the cost of the vertical movements of the drone and that of the workers comparable, and in practice we concentrate on the 2D movements in the warehouse. So, we ignore the up-and-down movements of the drone (and the up-and-down movements of the worker along the stairs) and we assume that both the drone and the workers always follow the shortest 2D path between any two consecutive points in their paths.

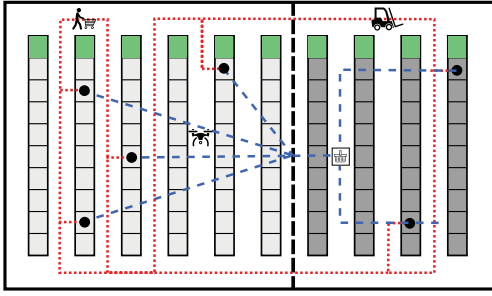


Fig. 2: A view from the top of the warehouse: the black dots are the positions of the items in a CO.

**Our Contributions:** The basic task for both the drone and the worker is to efficiently process COs. In this paper, we introduce the 2D *EM-grid* to represent the warehouses, and we define the picking problem on a CO for human workers and for drones. Due to the different payload constraints, the picking problem for humans reduces to a metric TSP among the positions of the items in the order. The picking problem for drones searches the optimal point inside the warehouse that minimizes the sum of the distances traversed by the drone to collect the items in the order. We propose three heuristics, called C-M-ALL, C-E-MB, and MIN-2C, to efficiently determine a sub-optimal solution for the drone picking problem. We give approximation bounds, and we evaluate via simulations their performance on the average case. Finally, we compare the drone and the worker picking system under the same conditions to derive the maximum number of items for which the drone system is profitable compared to the worker one.

The rest of the paper is organized as follows: In Sec. II, we introduce the warehouse mixed-grid model, the distance definitions for the drone and worker systems, the picking problem, and some properties. In Sec. III, we propose four different

efficient heuristics for the picking problem. In Sec. IV, we provide an extensive simulation evaluation in two possible scenarios. Conclusions and future works are offered in Sec. V.

## II. PROBLEM DEFINITION

### A. The warehouse model

We first define the *Euclidean-Manhattan-Grid* (*EM-grid*) which models the items position. This area is defined as a 2-dimensional grid  $G = (R, C, K)$  which consists of  $R$  rows,  $C$  columns (lanes), and a column parameter  $K \in [1, C]$  (which defines the *Border*  $B$ ) that separates the *Euclidean* grid  $E$  (i.e., the low cabinet area) from the *Manhattan* grid  $M$  (i.e., the high open-rack area). Specifically (as shown in Fig. 3):

$$\begin{aligned} E &= \{1, \dots, R\} \times \{1, \dots, K\} \\ B &= \{1, \dots, R\} \times \{K\} \subseteq E \\ M &= \{1, \dots, R\} \times \{K+1, \dots, C\} \end{aligned}$$

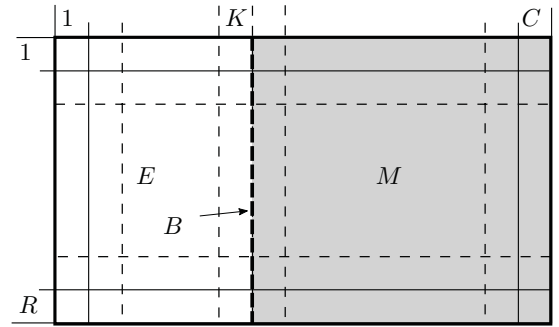


Fig. 3: The *EM-grid*.

As said before, we assume that the distance between any two pairs of consecutive vertices on the same row or column is constant, and for simplicity, we consider it unitary.

The border  $B$  consists of the single column  $K$ . Conventionally, the area consists only of low cabinets if  $K = C$ , and when  $K = 1$ , the warehouse consists entirely of high open-racks. In an *EM-grid*, any internal vertex  $u = (r_u, c_u)$  of  $G$ , i.e., with  $1 < r_u < R$  and  $1 < c_u < C$ , is connected to the four adjacent vertices  $(r_u, c_u \pm 1)$  and  $(r_u \pm 1, c_u)$ ; whereas, in general, any vertex of the grid, i.e., with  $1 \leq r_u \leq R$  and  $1 \leq c_u \leq C$ , is connected only to the existing adjacent vertices (i.e., an external node has only three or two neighbors).

### B. The possible moves and the distances

As explained, the drone moves following either straight lines when it moves among cabinets or the Manhattan distance when it moves among open-racks; whereas, the worker can only change lane at the bottom/top of the warehouse and it can move in the aisles.

1) *Drone's distance*: For any two vertices  $u, v$  in  $G$ , the distance  $d^D(u, v)$  is the length of the shortest path traversed by the drone in the  $EM$ -grid to go from  $u = (r_u, c_u)$  to  $v = (r_v, c_v)$ . Recalling that the Euclidean and Manhattan distances are defined, respectively, as:

$$d_E^D(u, v) = \sqrt{(r_u - r_v)^2 + (c_u - c_v)^2}$$

$$d_M^D(u, v) = |r_u - r_v| + |c_u - c_v|,$$

then, the distance  $d^D(u, v)$  for  $u, v \in G$  is given by:

$$d^D(u, v) = \begin{cases} 2d_E^D(u, v) & \text{if } u, v \in E \\ 2d_M^D(u, v) & \text{if } u, v \in (M \cup B) \\ 2 \min_{w \in B} \{d_E^D(u, w) + d_M^D(w, v)\} & \text{if } u \in E, v \in M \\ d^D(v, u) & \text{if } u \in M, v \in E \end{cases}$$

where the multiplicative constant 2 is due to the fact that the drone always makes a round trip and  $d^D(u, v) = d^D(v, u)$  because both Euclidean and Manhattan distances are symmetric.

By Lemma 1, the shortest path  $d^D(u, v)$  is unique and passes through the node in row  $v$  on the border  $B$ .

**Lemma 1** ([9]). *Consider an EM-Grid  $G = (R, C, K)$ . Given  $u = (r_u, c_u) \in E$  and  $v = (r_v, c_v) \in M$ , then  $d^D(u, v) = d_E^D(u, h) + d_M^D(h, v)$  with  $h = (r_v, K)$ .*

Thus, from now on,  $d^D(u, v)$  is finally given by:

$$d^D(u, v) = \begin{cases} 2d_E^D(u, v) & \text{if } u, v \in E \\ 2d_M^D(u, v) & \text{if } u, v \in (M \cup B) \\ 2(d_E^D(u, h) + d_M^D(h, v)) & \text{if } u \in E, v \in M \\ & \text{where } h = (r_v, K) \in B \\ 2(d_M^D(u, h) + d_E^D(h, v)) & \text{if } u \in M, v \in E \\ & \text{where } h = (r_u, K) \in B \end{cases} \quad (1)$$

2) *Worker's distance*: For any two vertices  $u = (r_u, c_u)$ ,  $v = (r_v, c_v)$  in  $G$ , the distance  $d^W(u, v)$  is the length of the shortest path traversed by the worker in the  $EM$ -grid to go from vertex  $u$  to  $v$ . Since the worker cannot cross either a cabinet or an open-rack, he/she needs to go to the end of the current aisle or to come back to the beginning of the aisle. According to this simple rule, it holds:

$$d^W(u, v) = \begin{cases} |r_u - r_v| & \text{if } c_u = c_v \quad (2a) \\ r_u + r_v + |c_u - c_v| & \text{if } c_u \neq c_v \quad (2b) \\ & \text{and } r_u + r_v \leq R \\ 2R - r_u - r_v + |c_u - c_v| & \text{if } c_u \neq c_v \quad (2c) \\ & \text{and } r_u + r_v > R \end{cases}$$

### C. The picking problem

The basic task in a warehouse is to serve a CO, i.e., to collect the required items from the shelves to satisfy a

customer. We denote this as the *picking problem* and our goal is to minimize the distance traveled to solve such problem.

A *customer-order*  $O = \cup_{i=1}^m \{u_i^{(n_{u_i})}\}$  consists of  $m$  distinct items, denoted as  $u_i$ , with  $i = 1, \dots, m$ , each with multiplicity  $n_{u_i} \geq 1$ . That is,  $n_{u_i}$  multiple copies of the same item  $u_i$  are required by the final user in  $O$ . Overall, the order  $O$  consists of  $n = \sum_{i=1}^m n_{u_i}$  items. For each item, we are interested in its position in  $G$ . So from now on, with abuse of notation, we denote also the item position with  $u_i$ . Let  $O_E$  be the subset of items which reside in  $E$ , and  $O_M$  the subset of items which reside in  $M$ . Clearly,  $O = O_E \cup O_M$ . Moreover, let  $n_E = \sum_{u \in O_E} n_u$  and  $n_M = \sum_{u \in O_M} n_u$ .

Given as input the CO  $O$ , the order in which the items are picked is important to minimize the distance traveled for the human worker. Namely, the best solution for the worker, who can drop the collected items one after the other in the cart that he/she pushes, is to find the cycle of minimum length that connects all the distinct vertices in  $O$ . That is, the picking problem for the worker reduces to the Traveling Salesman Problem (TSP).

For the drone, since it is almost impossible for it to collect more than one item at a time due to the grabbing difficulties mentioned above, the picking order does not impact the traveled distance. It is instead important to select a gathering point from which the drone goes back-and-forth to collect the items. We denote the gathering point also as the *drone's cart*. Hence, the picking problem is solved by searching for the gathering point that minimizes the sum of the distances between such a point and the items to be collected.

Fig. 2 illustrates feasible solutions for the picking problem, one for the drone and one for the worker. The order  $O$  is represented by the black dots. Recalling that the illustrated warehouse has 6 low lanes (light gray) and 4 high lanes (dark gray), and having set the drone's cart in the  $M$  area, the drone traverses the blue dashed lines. The worker, instead, follows the red dotted line.

The picking problem for the drone is formulated as follows. Given a CO  $O \subset G = (R, C, K)$ , let the *cost function* of the picking problem applied to  $O$  having set the gathering point at  $u \in G$  be:

$$\mathcal{C}(R, C, K, O, u) = \sum_{v \in O} n_v d^D(v, u) \quad (3)$$

that is, the cost is the sum of the distances between any item  $v \in O$  and the point  $u$ . Then, the picking problem looks for the point  $u^*$  that minimizes the cost function

$$u^* = \arg \min_{u \in G} \mathcal{C}(R, C, K, O, u) \quad (4)$$

Let  $u^* = (r^*, c^*)$  be the *gathering* (cart) point.

Note that, in our model, the drone and the worker deal with the multiplicity in a completely different way: while the drone has to go back-and-forth as many times as the multiplicity of the item, the worker stands in front of the item until he/she has collected all the required copies. So the multiplicity penalizes the drone.

From now on, when the warehouse parameters and customer order  $(R, C, K, \text{ and } O)$  are clear from context, we denote  $\mathcal{C}(R, C, K, O, u)$  as  $\mathcal{C}(u)$ . We first prove an interesting property for the picking problem of a CO with  $n = 2$ .

**Lemma 2.** Consider  $G = (R, C, K)$ . Given the CO  $O = \{u^{(n_u)}, v^{(n_v)}\}$ , then the gathering point  $u^*$  belongs to the shortest path between  $u$  and  $v$ .

*Proof.* First, we select a vertex  $q \in G$  that does not belong to the shortest path between  $u$  and  $v$ . W.l.o.g., let  $n_u \geq n_v$ . Let  $p$  be the vertex of the shortest path such that  $d^D(u, p) = d^D(u, q)$ . Then, the cost  $\mathcal{C}(q)$  of the picking problem setting the cart at  $q$  yields:

$$\begin{aligned} \mathcal{C}(q) &= n_u d^D(u, q) + n_v d^D(q, v) \\ &= n_u d^D(u, q) - n_v d^D(u, q) + n_v d^D(u, q) + n_v d^D(q, v) \\ &= (n_u - n_v) d^D(u, q) + n_v (d^D(u, q) + d^D(q, v)) \\ &\geq (n_u - n_v) d^D(u, q) + n_v d^D(u, v) \\ &= (n_u - n_v) d^D(u, p) + n_v d^D(u, v) \\ &= n_u d^D(u, p) + n_v (d^D(u, v) - d^D(u, p)) \\ &= n_u d^D(u, p) + n_v d^D(p, v) = \mathcal{C}(p) \end{aligned}$$

Hence, selecting any point  $q$  outside the shortest path is not convenient.  $\square$

Moreover, we observe that, for  $O = \{u^{(n_u)}, v^{(n_v)}\}$  if  $n_u = n_v \geq 1$ , then, any point  $p$  along the shortest path between  $u$  and  $v$  can be the gathering point.

When  $n_u > n_v$ , the best position of the cart is  $u$ , i.e., the vertex with the largest multiplicity. Namely, for any point  $p$ , with  $p \neq u$  along the shortest path between  $u$  and  $v$ , it yields:

$$\begin{aligned} \mathcal{C}(p) &= n_u d^D(u, p) + n_v d^D(p, v) \\ &= n_u d^D(u, p) + n_v d^D(u, v) - n_v d^D(u, p) \\ &= n_v d^D(u, v) + (n_u - n_v) d^D(u, p) > n_v d^D(u, v) = \mathcal{C}(u) \end{aligned}$$

In the following, we propose three heuristics for the drone picking system and one for the worker picking system.

### III. ALGORITHMS FOR THE PICKING PROBLEM

In this section, we first consider a warehouse with only low cabinets. In this case, the drone always moves in straight lines. Then, we study the general case, and provide heuristics to solve the picking problem, along with some approximation bounds. The picking problem for human workers is solved applying the well-known Christofides algorithm [10] after proving that the worker distance  $d^W$  is a metric.

#### A. Warehouse with only Low Cabinets

1) *The C-E-ALL Algorithm:* When the warehouse consists of only low shelves, the *EM-grid* grid reduces to a pure Euclidean grid with  $K = C$ . In this case, the cart point  $u^*$  defined in Eq. (4) is known in the literature as the *geometric median* [11]. No explicit formula nor an exact algorithm involving only arithmetic operations and  $k$ -th roots can exist in general for the geometric median [12]. The geometric

median can be approximated with iterative methods, like the Weiszfeld's algorithm [13]. More sophisticated geometric optimization procedures for efficiently finding approximated solutions to this problem have been given in [14] and in [15].

However, a good approximation for the gathering point known in the literature is the *centroid*, which is the arithmetic mean position of all the input points. The centroid  $C_{E-ALL}$  is the point that minimizes the sum of squared Euclidean distances between itself and each point in the set [16], thus we can approximate the optimum point  $u^*$  of  $O$  with  $C_{E-ALL}$ . To be more precise, given a CO  $O \in G$  in a pure Euclidean grid  $G = (R, C, C)$  (obviously,  $O = O_E$  and  $n = n_E$ ), the centroid  $C_{E-ALL}$  of  $O$  is the vertex:

$$C_{E-ALL} = \left( \frac{\sum_{u \in O} n_u r_u}{n_E}, \frac{\sum_{u \in O} n_u c_u}{n_E} \right). \quad (5)$$

The C-E-ALL algorithm selects  $C_{E-ALL}$  as the cart point for the drone. Moreover, according to Eq. (5),  $C_{E-ALL}$  can be computed in  $O(n_E)$  time.

#### B. Warehouse with Low Cabinets and High Open-Racks

In a general warehouse's layout, the drone flies over the cabinets according to the Euclidean metric and through the open-racks according to the Manhattan metric.

1) *The C-E-MB Algorithm:* Given an order  $O = O_E \cup O_M$ , if the gathering point is selected in the Euclidean side, the drone must fly horizontally along the open-racks to reach and bring all the items of  $O_M$  on the border  $K$  (see Eq. (1)). To move the items of  $O_M$  to the border, the drone travels the distance  $H = \sum_{u \in O_M} (c_u - K)$ . Such a distance  $H$  is independent from the cart point selected in  $E$ . Let  $O'_M$  be the set  $O_M$  where each item  $u = (r_u, c_u)$  has been replaced by its projection  $u' = (r_u, K)$  on the border. One can see that to serve the order  $O$  costs  $H$  plus the cost of serving the order  $O' = O_E \cup O'_M$  in a pure Euclidean grid. Hence, the C-E-MB algorithm selects as the cart location for the drone the vertex:

$$C_{E-MB} = \left( \frac{\sum_{u \in O} n_u r_u}{n_E + n_M}, \frac{\sum_{u \in O_E} n_u c_u + \sum_{u \in O_M} n_u K}{n_E + n_M} \right), \quad (6)$$

where  $C_{E-MB}$  is the centroid of  $O'$ . Note that,  $C_{E-MB}$  can be computed in  $O(n_E + n_M)$ .

**Theorem 1.** The approximation ratio performing the C-E-MB algorithm is at least 2.

*Proof.* Suppose we have a configuration like the one illustrated in Fig. 4. The two vertices  $u$  and  $v$  on the same row have

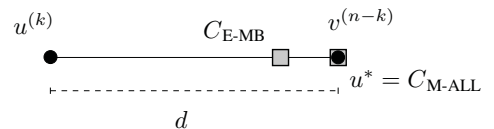


Fig. 4: The bad case of  $C_{E-MB}$ .

multiplicity  $k$  and  $n - k$ , respectively, with  $k \ll n$ . As



discussed before,  $u^* = v$ , while, by Eq. (6),  $C_{E-MB}$  is closer to  $v$  than  $u$ . The cost of the picking problem setting the cart at  $C_{E-MB}$  is  $k \left( \frac{n-k}{n} \right) d + (n-k) \left( \frac{k}{n} \right) d = 2k \left( \frac{n-k}{n} \right) d$ , while the optimal cost is  $kd$ . For large values of  $n$ , the ratio between this solution and the optimal solution tends to 2.  $\square$

Note that the same bound holds for the C-E-ALL in a pure Euclidean grid or a pure Manhattan grid because this configuration is feasible both either in  $E$  or  $M$ , and for two nodes on the same row  $d_E^D(u, v) = d_M^D(u, v)$ .

2) *The C-M-ALL Algorithm:* Consider a warehouse of only high open-racks. As discussed earlier the drone follows the Manhattan metric between any two vertices  $u$  and  $v$ . In this case, given an order  $O$ , the cart point  $u^*$  given in Eq. (4) is known in the literature as the *median* [9] and it will be denoted as:

$$C_{M-ALL} = (\tilde{r}_O, \tilde{c}_O) \quad (7)$$

where  $\tilde{r}_O$  and  $\tilde{c}_O$  are the median of the rows and the columns, respectively, of the items, up to multiplicities, in  $O$ . For example, given  $O = \{(1, 5), (1, 3), (4, 7)^2, (3, 2)\}$ ,  $C_{M-ALL} = (3, 5)$ .

We can use the median  $C_{M-ALL}$  as the gathering point of an arbitrary warehouse. Essentially, the C-M-ALL algorithm ignores the border that separates the Euclidean and the Manhattan side, and fixes the cart point for the drone at  $C_{M-ALL}$  as if the warehouse were  $G = (R, C, 1)$ . As the previous algorithms,  $C_{M-ALL}$  can also be computed in linear time [17].

**Theorem 2.** *The approximation ratio performing the C-M-ALL algorithm is at least  $\sqrt{2}$ .*

*Proof.* Suppose to have a configuration like the one illustrated in Fig. 5. The three vertices  $u = (0, 0)$ ,  $v = (d, d)$ , and  $z =$

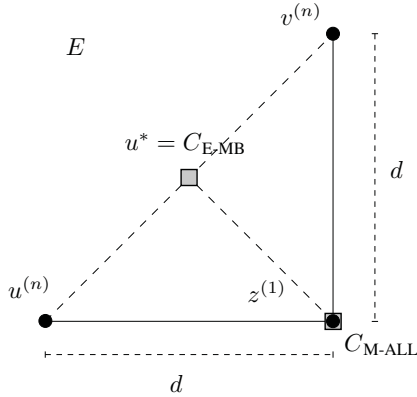


Fig. 5: The bad case of  $C_{M-ALL}$ .

$(d, 0)$  belong to the Euclidean part  $E$  of the  $EM$ -grid  $G$ . Each of the two vertices  $u$  and  $v$  have multiplicity  $n$ , while the third vertex has a single multiplicity. If  $n = 1$ , the gathering point is the *Fermat point*, which falls inside the triangle [18]. For large values of  $n$ , the gathering point is attracted by the straight line  $\overline{uv}$ . However, not all the points on  $\overline{uv}$  are optimal because of  $z$ . The closest point to  $z$  in  $\overline{uv}$  is the middle point  $\left( \frac{r_u + r_v}{2}, \frac{c_u + c_v}{2} \right) = \left( \frac{d}{2}, \frac{d}{2} \right)$ . Hence,  $u^* = \left( \frac{d}{2}, \frac{d}{2} \right)$  and  $\mathcal{C}(u^*) =$

$\frac{d}{2}\sqrt{2} + nd\sqrt{2}$ . Moreover,  $C_{M-ALL} = z$  for any value of  $n$  and  $\mathcal{C}(z) = 2nd$ . Thus, for large values of  $n$ ,  $\frac{\mathcal{C}(z)}{\mathcal{C}(u^*)} = \sqrt{2}$ .  $\square$

It is interesting to observe that, the configuration in Fig. 4 has  $u^* = C_{M-ALL}$ , whereas that in Fig. 5 has  $u^* = C_{E-MB}$ , when  $n$  is very large. This suggests a new algorithm that we call MIN-2C which selects as gathering point:

$$C_{\text{Min-2C}} = \arg \min \{ \mathcal{C}(C_{E-MB}), \mathcal{C}(C_{M-ALL}) \}.$$

Finally, we introduce two other points to be used in the last theorem. Given a CO  $O = O_M \cup O_E$  and the associated order  $O' = O'_M \cup O_E$ , where  $O'_M$  is the projection of the nodes in  $M$  on the border  $K$  as defined in the description of Algorithm C-E-MB, let  $C_{E-MB}^*$  be the geometric median of  $O'$ . Moreover, let  $C_M = (\tilde{r}_{O_M}, \tilde{c}_{O_M})$  be the median of the subset of points which belong to  $O_M$ , that is,  $\tilde{r}_{O_M}$  and  $\tilde{c}_{O_M}$  are the median of the rows and of the columns, respectively, of the items, up to multiplicities, of  $O_M$ .

We can also observe that, if  $u^*$  belongs to  $M$ , the column of  $u^*$  cannot be larger than the column of  $C_{M-ALL}$ , which is smaller than  $C_M$ . Unfortunately, we do not know a-priori when  $u^*$  resides in  $M$ . However, according to Theorem 3, we can circumscribe the position of  $u^*$  inside  $M$ .

**Theorem 3.** *The column  $c^*$  of  $u^*$  falls between the columns of  $G_{E-MB}^*$  and  $C_M$ .*

*Proof.* Suppose  $u^* = (r^*, c^*)$  belongs to  $M$ , and  $c^* > \tilde{c}_{O_M}$ . In  $O_M$ , there are at least as many items with column number less than  $c^*$ , as the number of items with column number greater than  $c^*$ . Thus, relatively to  $O_M$ , the cost at  $C_M$  is at most the cost at  $u^*$ . Nonetheless, for each item in  $O_E$ , the cost at  $C_M$  is less than the cost at  $u^*$ . Thus the overall cost at  $u^*$  is more than that at  $C_M$ .

When  $u^*$  belongs to  $E$ , the cost of  $O$  is the same as that of  $O'$  plus a fixed cost that corresponds to the cost paid to project on the border the items of  $O_M$ . Since the geometric median  $G_{E-MB}^*$  is the optimal solution for  $O'$ , it is not advantageous to shift  $u^*$  on the left of  $G_{E-MB}^*$ .  $\square$

**Theorem 4.** *The MIN-2C algorithm provides a  $\sqrt{2}$ -approximation ratio for the drone picking problem on EM-grids.*

*Proof.* The cost approximation ratio satisfies:

$$\frac{\mathcal{C}(C_{\text{Min-2C}})}{\mathcal{C}^*(u^*)} \leq \frac{\mathcal{C}(C_{M-ALL})}{\mathcal{C}^*(u^*)}.$$

When the gathering point is set to  $u^*$ , let  $\mathcal{C}_M(u^*)$  be cost of drone picking problem if  $G = (R, C, 1)$ , i.e., a fully Manhattan, and  $\mathcal{C}_E(u^*)$  be cost of drone picking problem if  $G = (R, C, C)$ , i.e., a fully Euclidean. Since  $d_E^D(u, v) \leq d_M^D(u, v)$ , then  $\mathcal{C}(C_{M-ALL}) \leq \mathcal{C}_M(C_{M-ALL})$  and  $\mathcal{C}^*(u^*) \geq \mathcal{C}_E(u^*)$ . By the optimality of  $C_{M-ALL}$  for a full Manhattan grid, one has  $\mathcal{C}_M(C_{M-ALL}) \leq \mathcal{C}_M(u^*)$ . Recalling the Cauchy-Schwarz inequality, that is,  $a + b \leq \sqrt{2}\sqrt{a^2 + b^2}$ , one has  $d_E^D(u, v) \leq d_M^D(u, v) \leq \sqrt{2}d_E^D(u, v)$  and therefore:

$$\frac{\mathcal{C}(C_{\text{Min-2C}})}{\mathcal{C}^*(u^*)} \leq \frac{\mathcal{C}(C_{M-ALL})}{\mathcal{C}^*(u^*)} \leq \frac{\mathcal{C}_M(u^*)}{\mathcal{C}_E(u^*)} \leq \sqrt{2}. \quad \square$$

3) *The TSP-W Algorithm:* Concerning the worker, as illustrated in Fig. 2, he/she travels inside the warehouse aisle by aisle. Since he/she is not constrained by any payload issue thanks to the cart, he/she can fulfill the entire CO traveling the cycle of minimum cost which connects all the vertices in  $O$ . The generic version of TSP is an  $NP$ -hard problem. Unless  $P = NP$ , there does not exist any polynomial-time approximation scheme for this generic problem [19].

**Lemma 3.** *The worker's movement  $D^W$  is a metric.*

*Proof.* Let  $u = (r_u, c_u)$ ,  $v = (r_v, c_v)$ , and  $z = (r_z, c_z)$  be any three vertices in  $G$ . From Eq. (2a), it is easy to see that  $d^W(u, u) = 0$ . Moreover, from Eq. (2c), both the non-negativity constraint (i.e.,  $d^W(u, v) \geq 0$ ) and the symmetry constraint (i.e.,  $d^W(u, v) = d^W(v, u)$ ) easily hold.

For the triangle inequality  $d^W(u, v) + d^W(v, z) \geq d^W(u, z)$ , we start considering the case when  $c_u \neq c_v \neq c_z$  and  $r_u + r_v \leq R$  and  $r_v + r_z \leq R$ . In this case, all the three vertices are under the sub-case specified in Eq. (2b). That is, recalling the triangle inequality applied to the absolute value function, i.e.,  $|x| + |y| \geq |x + y|$ , we obtain:

$$\begin{aligned} d^W(u, v) + d^W(v, z) &= \\ r_u + r_v + |c_u - c_v| + r_v + r_z + |c_v - c_z| &\geq \\ 2r_v + r_u + r_z + |c_u - c_z| &\geq \\ r_v + r_z + |c_u - c_z| &= d^W(u, z) \end{aligned}$$

The remaining cases can be proved in a similar way.  $\square$

Since the worker's movement is a *metric*, we can approximate the metric TSP by the Christofides algorithm [10].

So, we solve the TSP-W algorithm using the Christofides algorithm applied to the items in each CO: it gives an approximation factor of  $\frac{3}{2}$  in  $O(n^3)$  time, where  $n$  is the number of items in the CO [20]. We also compare the Christofides cycle with the optimum solution of the TSP, that we denote as TSP-OPT, obtained by a branch-and-bound implementation of the brute-force algorithm [19]. Obviously, although TSP-OPT returns the best cycle, it can become practically infeasible already for small values  $n$ . As we will see, in practice for our instances, the TSP-W algorithm returns solutions almost as good as TSP-OPT.

#### IV. SIMULATION EVALUATION

In our simulations, we consider an  $EM$ -grid  $G = (R, C, K)$ , with the number of columns  $C$  fixed to 100, and the number of rows  $R = \{30, 50, 70\}$ . To model different warehouse scenarios we set:  $K = 33$ , high open-racks dominate the area;  $K = 50$ , low cabinets and open-racks are evenly distributed;  $K = 66$ , low cabinets dominate; finally, we also consider a full low warehouse setting  $K = 1$ . We generate COs formed by  $5 \leq n \leq 25$  items, and the multiplicity of each item may vary from 1 to 5.

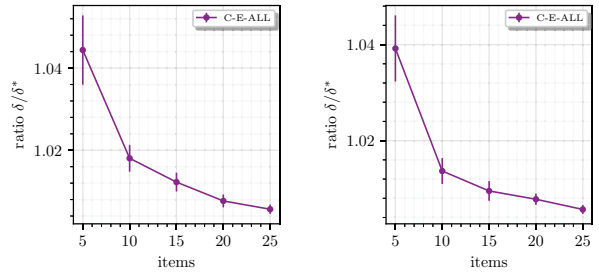
Our goal is to compare the performance of a picking system equipped with a drone with the performance of a traditional picking system where humans work. In Sec. IV-A, we compare

C-E-ALL with TSP. In Sec. IV-B, we first compare the drone heuristics among themselves, and then with TSP.

We generate 100 different random COs for each value of  $n$ . For each order, the optimal cost in Eq. (3) is computed by a brute-force algorithm for the drone picking problem, and by a branch-bound algorithm for the exact TSP [21]. The average value of the optimal exact cost for the picking problem and the average value of the costs computed using the algorithms proposed in Sec. III are denoted by  $\delta^*$  and  $\delta$ , respectively. We plot the average approximation ratio  $\frac{\delta}{\delta^*}$ , along with its 95% confidence interval.

##### A. Warehouse with only Low Cabinets

In this very first simulation, we consider a pure Euclidean grid, so the drone can fly over the shelves in straight lines. When the map is completely Euclidean, we can easily determine the centroid  $C_{E-ALL}$  invoking the C-E-ALL algorithm.

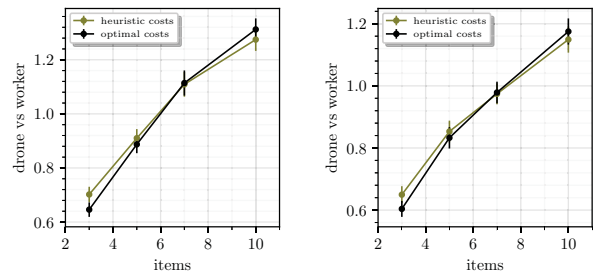


(a)  $R = 50$ .

(b)  $R = 70$ .

Fig. 6: Ratio  $\frac{\delta}{\delta^*}$  in an Euclidean grid when  $C = 100$  and  $R$  varies.

In Fig. 6, it is worthy to note that C-E-ALL improves when the number of items  $n$  increases. This also means that the centroid is a good approximation of the geometric median already when  $n = 25$ . However, one has to recall that the approximation can be 2 (see Theorem 1) or even larger.



(a)  $R = 50$ .

(b)  $R = 70$ .

Fig. 7: The ratio between the average distance traveled by the drone and that by the worker using either the two heuristics C-E-ALL and TSP-W or the two optimal solutions, when  $C = 100$  and  $R$  varies.

In Fig. 7, we compare the performance of the drone picking system with the performance of the traditional picking system. When the curve is below 1, the drone is more profitable than a human worker; and vice versa, when the curve is above

1, the traditional warehouse beats the drone. In general, as expected, the drone beats the human worker when  $n$  is small because when  $n$  is large the human can amortize the traversed distance over the number of items he/she collects. Instead, due to the payload constraint, the drone traverses the same distance multiple times to collect a given item, independent of the total number of items it collects. Increasing the value of  $R$ , since the length of the worker path increases, the drone beats the worker for slightly larger values of  $n$ . Moreover, since the ratio between the average cost of the optimal solutions for the drone and for the workers is almost coincident with the ratio of the heuristics, we have evidence that the heuristics do not substantially change the performance of the picking systems. We can conclude that the drone is more profitable when the orders have items with multiplicity one, while the traditional picking system is more profitable when items in an order have multiplicity greater than one.

### B. Warehouse with Low Cabinets and High Open-Racks

1) *Algorithm performance:* In this scenario the *EM*-grid is mixed, hence the movement of the drone is constrained by the shelves. In Fig. 8 we plot the comparison of the three heuristics C-E-MB, C-M-ALL, and MIN-2C, with respect to the optimum algorithm OPT which computes  $u^*$ , i.e., the value that minimizes the objective cost function in Eq. (4) computed by a brute-force algorithm.

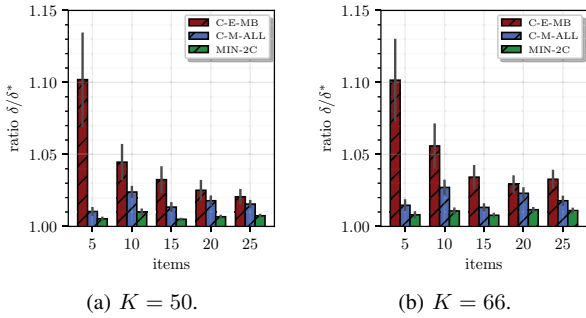


Fig. 8: Ratio  $\frac{\delta}{\delta^*}$  when  $R = 50$ ,  $C = 100$ , and  $K$  varies.

As expected, MIN-2C is the best algorithm recalling the  $\sqrt{2}$ -approximation (see Theorem 4). Note that, since we are plotting the average costs of 100 experiments, the bar of MIN-2C does not coincide with the minimum between the bars  $C_{E-MB}$  and  $C_{M-ALL}$ . C-M-ALL is always better than C-E-MB.

All the heuristics, but C-E-MB for small values of  $n$ , are less than 3% away from the optimum value. As expected, C-M-ALL works better when  $K$  is small, and C-E-MB when  $K$  is large. The performance of C-E-MB depends particularly on the distribution of the items between the cabinets and the open-racks, as illustrated in Fig. 9. Since C-E-MB assumes that the gathering point resides in  $E$ , the performance of C-E-MB is poor (and approaches 2) when  $n_E = 1$ . Whereas, it strongly improves when the majority of the items are in  $E$ .

2) *Drone picking system vs Traditional picking system:* Finally, we compare the performance of a traditional picking

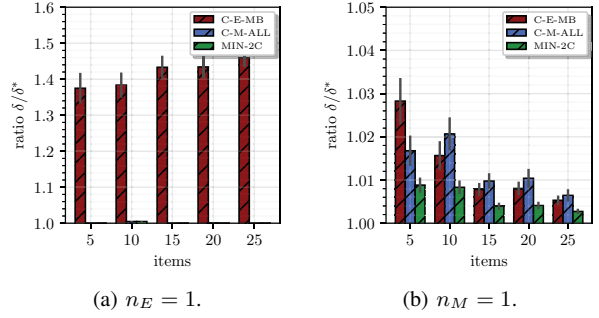


Fig. 9: Ratio  $\frac{\delta}{\delta^*}$  when  $R = 50$ ,  $C = 100$ , and  $K = 50$  varying  $n$ .

system with the performance of the picking system with drone in a mixed warehouse. Although the drone has to go back and forth each time from the cart point, when  $n$  is small, the path-length of the drone is less than the distance traveled, according to a TSP solution, by the worker. From the three plots in Fig. 10, we can see that when the number of rows  $R$  increases, the drone is more profitable an increasing number of items. Comparing the results in Fig. 7 and Fig. 10, although the distance traveled by the drone in mixed warehouses is longer than that in fully low warehouses, the drone still outperforms the worker for, approximately, the same number of items. Thus, again the drone efficiently handles multiplicity one orders, while the traditional system requires that multiple orders are handled in each TSP cycle.

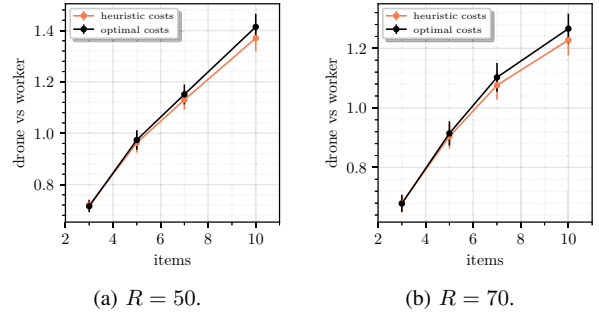
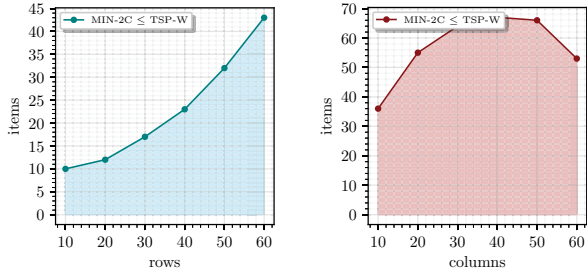


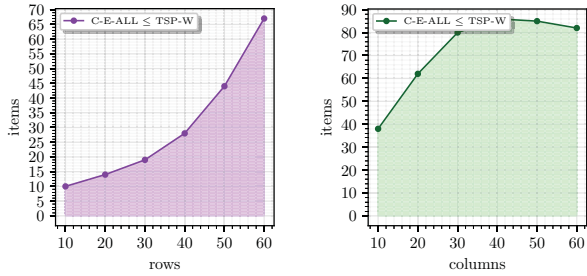
Fig. 10: The ratio between the average distance traveled by the drone and by the worker using either the two heuristics MIN-2C and TSP-W or the optimal solutions, when  $C = 100$ ,  $K = 50$ , and  $R$  varies.

### C. Time Performance

Up to now, we have analyzed when the drone system is profitable in terms of distance. It remains to observe that the drone flies at a speed which is at least three times the walking speed of the worker in the warehouse. Even if time penalties are introduced to collect items, it is reasonable to assume that the drone still remains about twice as fast as the worker in collecting items at the same distance. So we have reformulated the cost function in Eq. (3) in terms of time, replacing  $d^D(u, v)$  with  $t^D(u, v) = \frac{d^D(u, v)}{2}$ , but keeping the worker time as the previous distance, i.e.,  $t^W(u, v) = d^W(u, v)$ .



(a) MIN-2C,  $C = 100$ ,  $R$  varies. (b) MIN-2C,  $R = 50$ ,  $C$  varies.



(c) C-E-ALL,  $C = 100$ ,  $R$  varies. (d) C-E-ALL,  $R = 50$ ,  $C$  varies.

Fig. 11: Time ratio comparison: the colored area represents when the heuristic is faster than TSP-W.

In Fig. 11, we report on the maximum number of items for which the drone is more profitable than a worker. We evaluate when the average time cost for the drone using Algorithm MIN-2C is less than or equal to the average time cost for the worker using Algorithm TSP-W. For  $C = 100$  and  $K = 50$ , Fig. 11(a) shows that, when  $R$  increases but remains smaller than  $C$ , the drone is more profitable an increasing number of items. This means that under the same conditions, when  $R$  increases, the cost of TSP increases faster than the cost of the drone. Even more interesting is Fig. 11(b). When  $R = 50$ ,  $K = \frac{C}{2}$ , and  $C$  varies, the drone is more profitable an increasing number of items until  $C \leq R$ . When  $R \leq C$  and  $C$  increases, the number of items decreases, coherently, in some way, with Fig. 11(a). Our understanding is that, although the drone travels shorter distances than the worker, in high open-racks the gain  $d_M^D(u, v) - d^W(u, v)$  depends only on  $R$ , and thus decreases in percentage when  $R$  is fixed and  $C$  is large. However, this behavior is interesting and will require further investigations. Finally, Fig. 11(c) and Fig. 11(d) analyze when the drone is profitable in a pure Euclidean grid. In general, since in the Euclidean grid the drone traverses distances shorter than in  $EM$ -grids, the number of items up to which the drone is profitable is larger in Euclidean grids than in mixed-grids. With respect to the analysis of the time, the drone system becomes very competitive with the worker system.

## V. CONCLUSION

In this paper, we have introduced the picking problem for human workers and for drones, after modeling the warehouse as  $EM$ -grid and considering a very basic model for the worker

and drone movements. We have neglected the vertical movements and the effect of the payload on the human and drone movements, but it remains to consider a more sophisticated model for the movement that includes penalties for changing direction, climbing stairs, and payload. A deeper study of the 3D shortest distances is also interesting.

We have examined when the drone is more effective compared to the traditional solution that employs a worker pushing a cart in term of the size of the CO. It remains to quantify the advantage of the drone system that uses high open-racks with respect to low cabinets suitable for human workers on the level of occupancy of the warehouse.

A natural extension of this work is to consider a cooperative approach between humans and drones. Solutions with multiple drones sound quite challenging.

## REFERENCES

- [1] F. Betti Sorbelli, S. K. Das, C. M. Pinotti, and S. Silvestri, "Range based Algorithms for Precise Localization of Terrestrial Objects using a Drone," *Pervasive and Mobile Computing*, vol. 48, pp. 20–42, 2018.
- [2] F. Betti Sorbelli, C. M. Pinotti, and V. Ravelomanana, "Range-Free Localization Algorithm Using a Customary Drone: Towards a Realistic Scenario," *Pervasive and Mobile Computing*, vol. 54, pp. 1–15, 2019.
- [3] V. Olivares, F. Cordova, J. M. Sepúlveda, and I. Derpich, "Modeling internal logistics by using drones on the stage of assembly of products," *Procedia Computer Science*, vol. 55, pp. 1240–1249, 2015.
- [4] M. J. Gravier, E. Companik, I. Farris, and M. Theodore, "Feasibility of warehouse drone adoption and implementation," *Digital*, 2018.
- [5] T. Verge, "Welcome to the automated warehouse of the future," <https://goo.gl/jBULvR>, 2018, [Online; accessed 22-02-2019].
- [6] S.-J. Kim, D.-Y. Lee, G.-P. Jung, and K.-J. Cho, "An origami-inspired, self-locking robotic arm that can be folded flat," *Science Robotics*, vol. 3, no. 16, p. eaar2915, 2018.
- [7] T. Information, "Amazon developing picking robots for warehouses," <https://goo.gl/GRBK1l>, 2018, [Online; accessed 22-02-2019].
- [8] Z. Net, "Walmart's drone ambitions are real, and smarter than amazon's," <https://goo.gl/QqgAJy>, 2018, [Online; accessed 22-02-2019].
- [9] L. Bartoli, F. Betti Sorbelli, F. Corò, C. M. Pinotti, and A. Shende, "Exact and Approximate Drone Warehouse for a Mixed Landscape Delivery System," in *2019 IEEE SMARTCOMP (to appear)*, 6 2019.
- [10] N. Christofides, "Worst-case analysis of a new heuristic for the travelling salesman problem," Carnegie-Mellon Univ Pittsburgh Pa Management Sciences Research Group, Tech. Rep., 1976.
- [11] G. O. Wesolowsky, "The weber problem: History and perspectives," *Computers & Operations Research*, 1993.
- [12] C. Bajaj, "Proving geometric algorithm non-solvability: An application of factoring polynomials," *Journal of Symbolic Computation*, vol. 2, no. 1, pp. 99–102, 1986.
- [13] Z. Drezner and H. W. Hamacher, *Facility location: applications and theory*. Springer Science & Business Media, 2001.
- [14] P. Bose, A. Maheshwari, and P. Morin, "Fast approximations for sums of distances, clustering and the fermat-weber problem," *Computational Geometry*, vol. 24, no. 3, pp. 135–146, 2003.
- [15] M. B. Cohen, Y. T. Lee, G. Miller, J. Pachocki, and A. Sidford, "Geometric median in nearly linear time," in *Proceedings 48th annual ACM symposium on Theory of Computing*. ACM, 2016, pp. 9–21.
- [16] M. H. Protter and C. B. Morrey, *College calculus with analytic geometry*. Addison-Wesley, 1977.
- [17] T. H. Cormen, C. E. Leiserson, R. L. Rivest, and C. Stein, *Introduction to algorithms*. MIT press, 2009.
- [18] J. Haldane, "Note on the median of a multivariate distribution," *Biometrika*, vol. 35, no. 3-4, pp. 414–417, 1948.
- [19] S. Sahni and T. Gonzalez, "P-complete approximation problems," *Journal of the ACM (JACM)*, vol. 23, no. 3, pp. 555–565, 1976.
- [20] C. Nilsson, "Heuristics for the traveling salesman problem," *Linköping University*, pp. 1–6, 2003.
- [21] E. L. Lawler, J. K. Lenstra, A. R. Kan, D. B. Shmoys et al., *The traveling salesman problem: a guided tour of combinatorial optimization*. Wiley New York, 1985, vol. 3.